The performance of silicon detectors for the SiliPET project: A Small Animal PET Scanner based on Stacks of Silicon Detectors

Natalia Auricchio[a,c], Giovanni di Domenico[b,c], Guido Zavattini[b,c], Luciano Milano[b,c], Roberto Malaguti[c]

[a] *INAF/IASF, Bologna, Italy*
[b] *University of Ferrara, Dept. of Physics, Ferrara, Italy*
[c] *INFN-Ferrara, Ferrara, Italy*

Abstract

We propose a new scanner for small-animal Positron Emission Tomography (PET) based on stacks of double sided silicon detectors. Each stack is made of 40 planar detectors with dimension 60×60×1 mm^3 and 128 orthogonal strips on both sides to read the two coordinates of interaction, the third being the detector number in the stack. Multiple interactions in a stack are discarded by an exclusive OR applied between each detector plane of a stack. In this way we achieve a precise determination of the interaction point of the two 511 keV photons. The reduced dimensions of the scanner also improve the solid angle coverage resulting in a high sensitivity. Preliminary results were obtained with MEGA prototype tracker (11 double sided Si detector layers), divided into two stacks 2 cm apart made of respectively 5 and 6 prototype layers, placing a small spherical ^{22}Na source in different positions. We report on the results, spatial resolution, imaging and timing performances obtained with double sided silicon detectors, manufactured by ITC-FBK, having an active area of 3×3 cm^2, thickness of 1 mm and a strip pitch of 500 μm. Two different strip widths of 300 μm and 200 μm equipped with 64 orthogonal p and n strips on opposite sides were read out with the VATAGP2.5 ASIC, a 128-channel "general purpose" charge sensitive amplifier.

Key words: positron emission tomography, small animal, silicon detector

1. SiliPET scanner

The proposed small animal PET scanner is based on 4 stacks of double-sided silicon detectors [1]. Each stack is composed of 40 planar sensors with dimension 60×60×1 mm^3 and 128 orthogonal strips on both sides to permit the measurement of the two coordinates on the plane of the detector. The third coordinate, the depth of interaction, is given by the identification of the detector plane in which the interaction takes place with a precision determined by its thickness. This geometry is finalized to maximize the sensitivity, recovering the lines of response passing near to corners of the four stacks. The advantages of the proposed configuration are the accurate measurement of the position of interaction in the plane of the detector, selecting which strips have detected a photon, and the measurement of the depth of interaction by the element of the stack that contains these strips, with a precision determined by its thickness. An event is recorded when the strip signal exceeds the required energy threshold of 50 keV. All planes in a stack are in exclusive OR imposing therefore a single interaction. The capability of measuring the depth of interaction makes it possible to design a very compact scanner with large solid angle coverage. Furthermore due to the scanner compactness, non collinearity effects become negligible. The readout electronics can be simplified since the energy measurement is superfluous.

It is expected that the positron range dominates the ultimate spatial resolution.

2. Monte Carlo simulations

The simulations of the designed system were performed with EGSnrc code in order to estimate the spatial resolution and the sensitivity [2]. After a Compton interaction the recoil electron is transported and the deposited energy is registered when the low energy threshold of 50 keV is exceeded. In order to discard multiple interactions inside a stack, the signals from detectors composing a stack are connected with a logical exclusive OR operator so that a coincidence event is considered only if two detectors in two different stacks register a single plane. If two or more voxels (identified by the front and back strips and the detector plane) register a signal above threshold in a same plane, during the readout of the strips only the first one is registered: the system becomes a digital counter of hits. An isotropic point-like source of ^{18}F is placed at the center of the system emitting positrons. Surrounding it, a 1.5 cm radius cylinder of water was placed to simulate the positron interaction with the mouse body. Furthermore, in the annihilation process non-collinearity of two gamma-rays was included with a Gaussian distribution and a FWHM of 0.5°.

The profiles of a sinogram produced with the ^{18}F source are compared in Fig. 1 before and after considering the positron range effects. If the positron range is not included, the spatial resolution (FWHM) is 0.33 mm, due to the strip pitch, while in the case where the positron range is considered the FWHM enhances to 0.52 mm, dominated therefore by positron range. In Fig. 2 we report the absolute efficiency of the total system

as a function of detector stack thickness: a total thickness of 4 cm implies an efficiency of 5.1%, which compared to existing scanners is high.

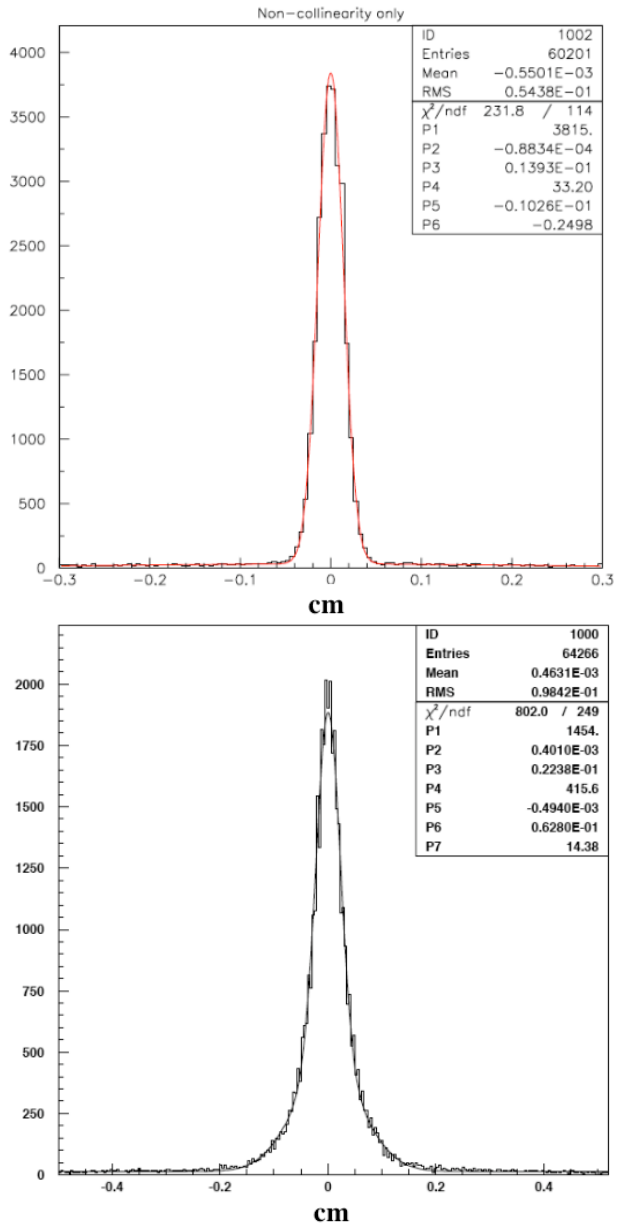

Figure 1: Profiles of a sinogram of a point-like ^{18}F source placed at the center of the scanner. *Top:* positron range effects have been neglected; *bottom:* positron range is included.

In Fig. 3 the SiliPET scanner performances are compared to those of current small animal PET scanners.

A proof of principle measurement was performed at the MPE, using the prototype tracker of the MEGA advanced Compton imager [3], composed of 11 double sided silicon detector layers. To simulate a silicon PET system the tracker is divided into two stacks 2 cm apart made of respectively 5 and 6 prototype layers and a small spherical ^{22}Na source is placed in 5 different positions. Each layer of the tracker is composed of a 3×3 array, each 60×60×0.5 mm^3 in size. Each wafer has

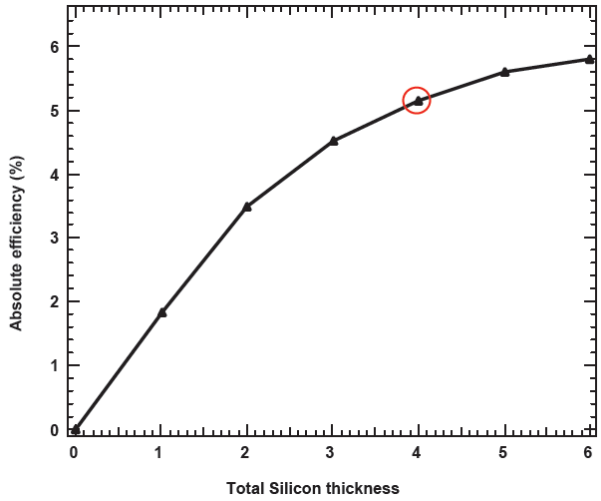

Figure 2: Absolute efficiency of the SiliPET scanner as a function of detector stack thickness.

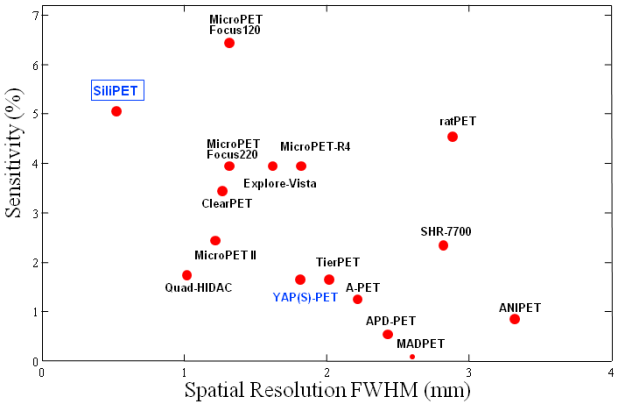

Figure 3: SiliPET scanner performances.

128 orthogonal p and n strips on opposite sides with a 470 μm pitch. The diameter of source is ~1 mm and the spatial resolution (FWHM) of the system is 0.95 mm. A detector spatial resolution at FWHM of 640 μm was obtained [4].

3. Measurements

We tested some double sided silicon strip prototype detectors, manufactured by ITC-FBK, characterized by a smaller active area of 3×3 cm^2, a strip pitch of 500 μm, strip widths of 300 μm and 200 μm, and thickness of 1 mm. Each detector is fitted with 64 orthogonal p$^+$ and n$^+$ strips on opposite sides. The wafers were produced from high resistivity n-type substrate: the values were measured within the range 15-30 kΩ cm. The p-side bias ring is surrounded by a wide guard ring in turn surrounded by ten narrow floating p$^+$ guard-rings designed to reduce the bias voltage applied from bias ring to the crystal cut edge. The strips are AC coupled on the wafer itself since the metal electrode runs over the strip with a decoupling dielectric layer in between.

Each sensor side was bonded to a VATAGP2.5 ASIC for strip readout [5].

We have performed an electrical characterization including the single strip and total leakage current measurements. Our goal was to verify the conformity of the detector characteristics to the SiliPET requirements. The detectors were tested on both sides. A reverse voltage ramp is applied at the n (p)-side bias line while measuring the current flowing at p (n)-side bias ring terminal kept at the ground potential. Bias-ring current includes the leakage current contribution of all strips, which are resistively connected to the bias ring via the punch-through effect. In Fig. 4 we report the total leakage current of the tested detectors equipped with strips 300 μm wide. We can note that the leakage current of wafer 1 is very high, while the breakdown voltage of the other detectors is quite uniform.

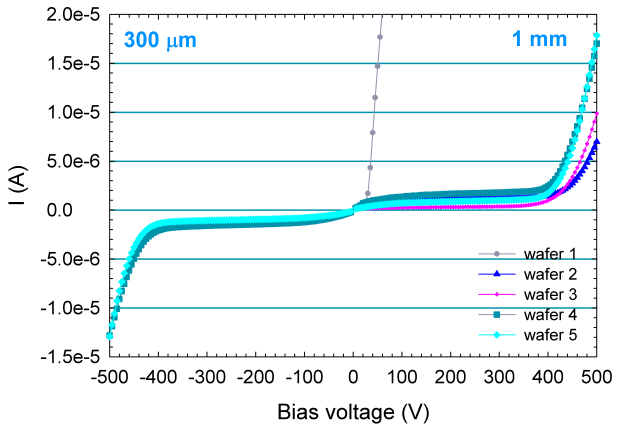

Figure 4: N and p-side total leakage currents measured using the 1 mm thick detectors equipped with strips 300 μm wide.

We have performed the single strip leakage current measurements: DC scans do not show any defective strip and AC scans present a negligible number of broken capacitors (~0.4%).

The low energy threshold should be below 50 keV, so as to acquire as many Compton events as possible without losing in efficiency. This parameter was measured evaluating the minimum energy relievable in the strip spectra of a ^{133}Ba source (see Fig. 5). The distribution of the energy threshold values measured for a sensor is shown in Fig. 6. An estimate of this value is ~25 keV.

3.1. Spatial resolution

A ^{22}Na spherical source was mounted on a 2-D positioning system controlled by micrometer screws and placed between two opposed silicon detectors in seven different positions. The source diameter is of ~1 mm. The spatial resolution was estimated using a simple planar back-projection algorithm. The profiles as a function of the source position on the silicon sensors at ± 0.5, 1 and 5 mm, with respect to a central strip, in the orthogonal direction to the strips present an average FWHM of 0.87 mm, including the source dimension. The FWHM spatial resolution is calculated by Gaussian fit of the distributions related to each position and the background was modeled by a Gaussian distribution. The detector intrinsic spatial resolution after subtracting the source dimension is 0.51 mm.

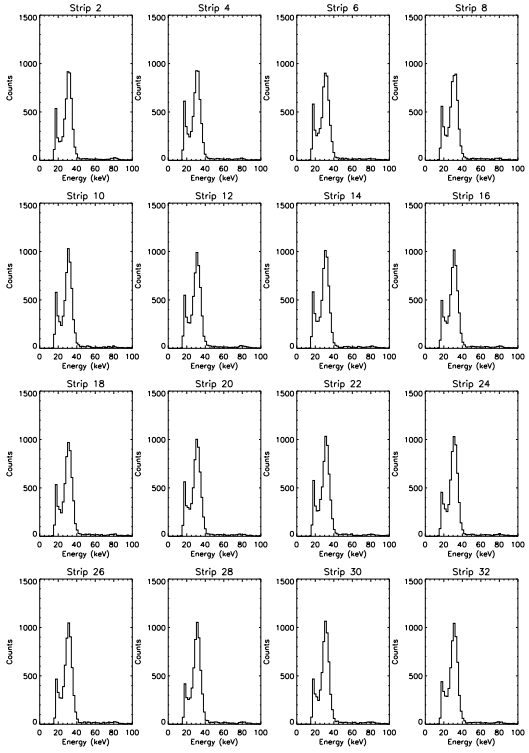

Figure 5: Example of spectra acquired by irradiating 16 different strips with ^{133}Ba.

3.2. Coincidence timing resolution

Timing measurements between two opposed silicon detectors were carried out using a ^{22}Na source placed at the center of the FOV, employing the same experimental setup used to evaluate the spatial resolution. The estimated time resolution (FWHM) is about 200 ns due to the amplitude walk. Using a dedicated ASIC circuit designed by the Politecnico of Milano for fast timing measurements we have obtained an improved resolution of 16.5 ns (FWHM). This was measured using a ^{22}Na radioactive source placed between a silicon detector and a YAP detector optically glued to a photomultiplier tube with constant fraction timing.

An amplitude walk correction method requires the acquisition of the timing signal and the pulse height in coincidence for each event. The experimental setup used for compensating the timing measurements is shown in Fig. 7. The time resolution before correcting was 128±3 ns, while after compensating it is 18±3 ns (see Fig. 8).

3.3. Imaging performance

The double sided microstrip detector response uniformity was investigated recording a 2-D image of a ^{57}Co uncollimated source and the illuminated sensor presents excellent response uniformity.

The resolution uniformity across the FOV was evaluated using a Pb mask 2 mm thick and equipped with the hole array shown in Fig. 9. We can see in Fig. 10 that the holes are well

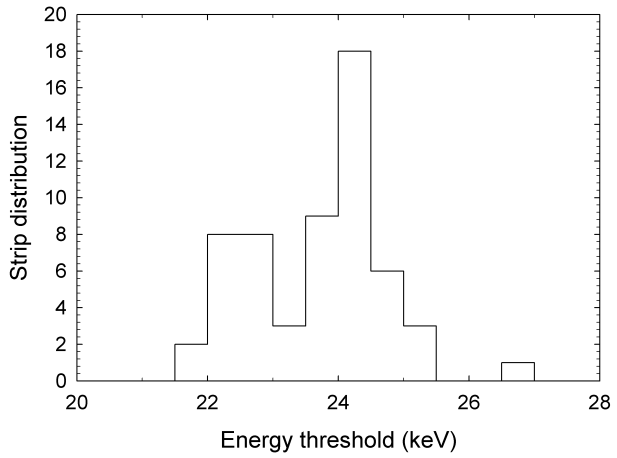

Figure 6: Energy threshold distribution.

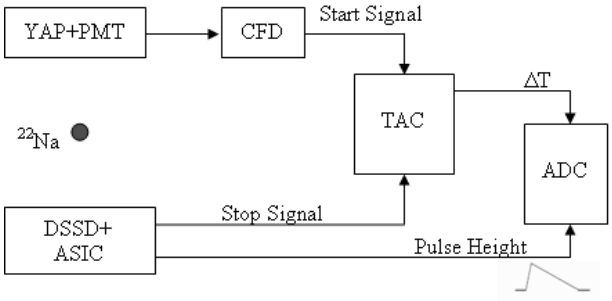

Figure 7: Block diagram of the experimental setup used for compensating the timing measurements.

resolved when the horizontal separation is greater than the strip pitch, concluding therefore that the spatial resolution of the detector is dominated by the strip pitch.

4. Conclusions

Our simulations have shown the good performance of a small animal PET scanner based on thick double-sided silicon detectors. Proof of principle measurements have confirmed the expected very high spatial resolution. We have measured an energy threshold better than 28 keV.

We have obtained an intrinsic spatial resolution <0.6 mm and a timing resolution of ~20 ns FWHM using either a custom ASIC designed by the Politecnico of Milano for fast timing measurements or amplitude walk correction methods.

References

[1] G. Zavattini et al., High Z and Medium Z Scintillators in Ultra-High-Resolution Small Animal PET, IEEE Trans. Nucl. Sci., vol. 52, no.1, pp. 222-230 (2005).

[2] G. Zavattini et al., SiliPET: An ultra high resolution design of a small animal PET scanner based on double sided silicon strip detector stacks, NIM A568, pp. 393-397 (2006).

[3] P. Bloser et al., Development of silicon strip detectors for a medium energy gamma-ray telescope, NIM A512, pp. 220-228 (2003).

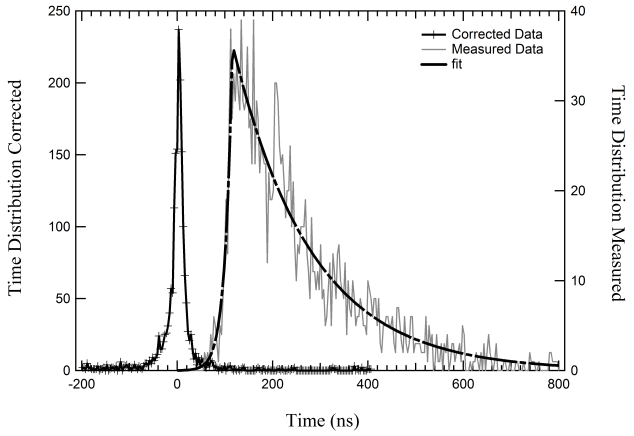

Figure 8: Comparison between the time spectrum before and after correction.

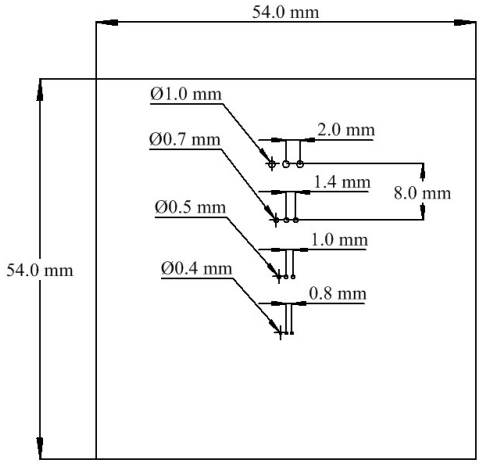

Figure 9: Schematic drawing (not in scale) of the Pb mask used to evaluate the spatial resolution.

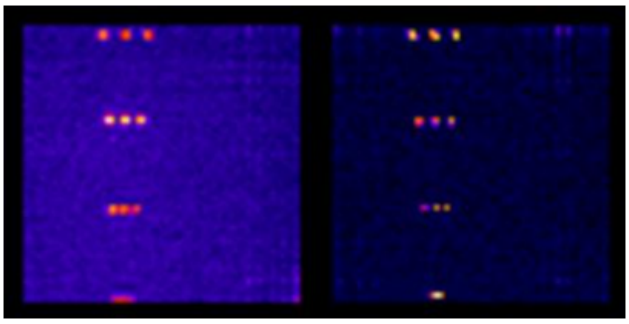

Figure 10: 2-D images recorded by irradiating the sensor through a Pb mask with ^{57}Co *(left)* and ^{241}Am *(right)*.

[4] G. Di Domenico, et al., SiliPET: An ultra-high resolution design of a small animal PET scanner based on stacks of double-sided silicon strip detector, NIMA 571, pp. 22-25 (2007).

[5] N. Auricchio, et al., First Measurements for the SiliPET project: A Small Animal PET Scanner based on Stacks of Silicon Detectors, IEEE Nuclear Science Symposium Conference Record, p. 2926 (2007)